Inorganic Chemistry Communications 101 (2019) 52–56

Contents lists available at ScienceDirect

Inorganic Chemistry Communications

journal homepage: www.elsevier.com/locate/inoche

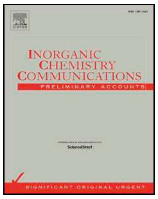

Short communication

A Zn(II)/anthracene coordination polymer showing highly efficient photocatalytic Cr(VI) reduction in aqueous solution

Jing Li[a], Wei Gou[b], Yan Zhou[c], Zhen-Fang Lin[d,*], Fei Peng[e,*]

[a] *School of Chemical Engineering, Xi'an University, Xi'an, Shaanxi, China*
[b] *Department of Neurology, The Seventh People's Hospital of Chengdu, Chengdu, Sichuan, China*
[c] *2nd TB Endemic Area, The Public Health Clinical Center of Chengdu, Chengdu, Sichuan, China*
[d] *Department of Neurology, Sichuan Provincial Rehabilitation Hospital Affiliated with Chongqing medical University & Sichuan Bayi Rehabilitation Center, Chengdu, Sichuan, China*
[e] *Department of Pharmacy, People's Hospital of Changshou Chongqing, Chongqing, China*

GRAPHICAL ABSTRACT

Reaction of $Zn(OAc)_2{\cdot}2H_2O$ with the visible light responsive organic ligand 9,10-bis(4′ -pyridylethynyl)-anthracene (BPEA) gave rise to a Zn(II)/anthracene coordination polymer with a one-dimensional (1D) chain structure. The as-prepared compound shows broad-range visible light absorption and good water stability, and could be applied as the photocatalyst with high efficiency and stability.

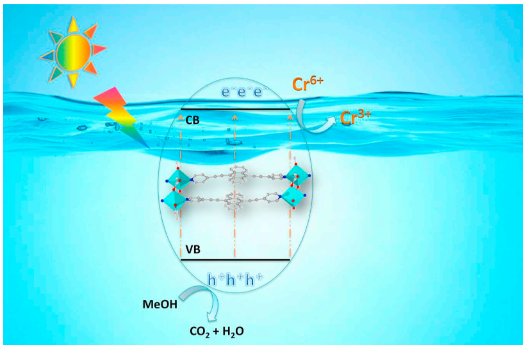

ARTICLE INFO

Keywords:
Coordination polymer
Anthracene-based ligand
Photocatalysis
Cr(VI) reduction

ABSTRACT

Reaction of $Zn(OAc)_2{\cdot}2H_2O$ with the visible light responsive organic ligand 9,10-bis(4′ -pyridylethynyl)-anthracene (BPEA) gave rise to a Zn(II)/anthracene coordination polymer $[Zn(OAc)_2(BPEA)]_n$. Compound **1** has a one-dimensional (1D) chain structure in which the binuclear $\{Zn_2(OAc)_2\}$ cores are linked by the BPEA ligands using the pyridyl N atoms to give to the 1D ladder-like network. The as-prepared compound **1** shows broad-range visible light absorption and good water stability, which are highly demandable for its application in the photocatalysis. The photocatalytic property of **1** were investigated by reduction of Cr(VI) to Cr(III) in aqueous solution under visible light, which reveals its high efficiency and stability in this photocatalytic process.

Nowadays, there is growing concern about environmental protection and human health because more and more areas of the earth are facing serious water pollution [1]. Among all the pollutants, heavy metals effluents from industrial discharge has awakened the public concern over the last decade because they are usually highly toxic which are not easy to be degraded biologically directly [2]. For instance, inorganic hexavalent chromium Cr(VI) is with high levels of toxicity and nonbiodegradable, and it could also cause DNA damage

---

* Corresponding authors.
E-mail addresses: zhenfang_lin666@yeah.net (Z.-F. Lin), fei_peng666@yeah.net (F. Peng).

https://doi.org/10.1016/j.inoche.2019.01.006
Received 8 December 2018; Received in revised form 3 January 2019; Accepted 4 January 2019

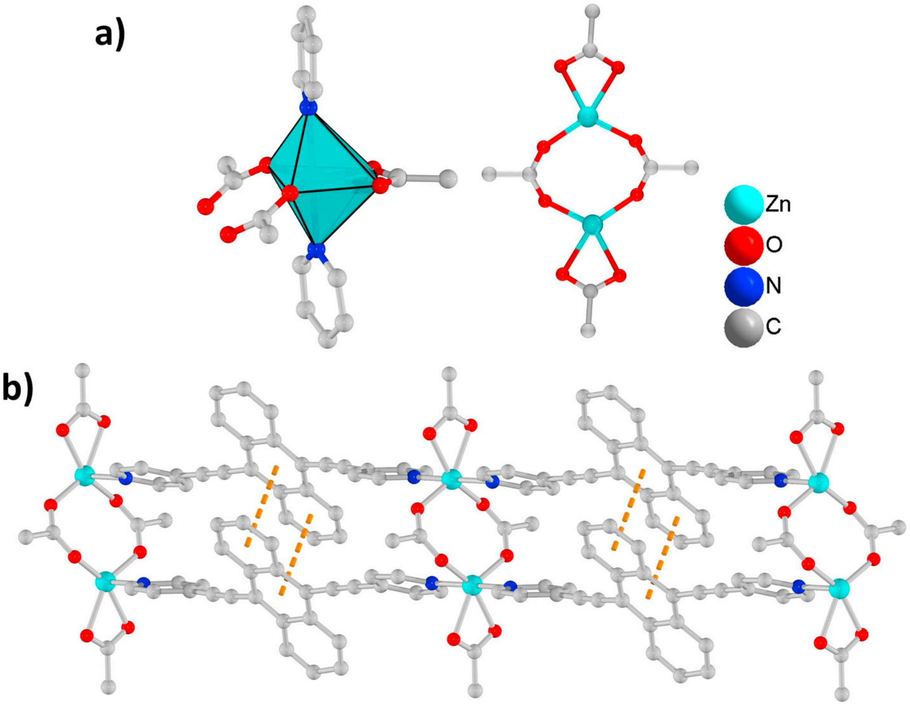

Fig. 1. (a) The coordination environment of the Zn(II) ion and the $\{Zn_2(AcO)_4\}$ unit; (b) The 1D chain-like network of **1** showing the π-π interactions.

and cancers. In comparison, Cr(III) is nontoxic and served as an essential trace metal for human health [3]. In this case, the reduction of Cr(VI) to Cr(III) is an effective method to reduce the toxicity of Cr(VI) to the environment and human beings. Reported studies categorize the reduction into three types: chemical reduction, microbial reduction and photocatalytic reduction [4–6]. Among them, the photocatalytic reduction under visible light is green and cost-effective for the wastewater treatment, due to the abundant visible light (50%) in the solar energy [7].

As an emerging class of crystalline hybrid material, coordination polymers (CPs) have undergone a booming development in the last ten years because they could be applied in various fields, including fluorescent materials and heterogeneous catalysis [8–17]. Some CPs show their semiconductors behavior under irradiation, implying that they are potentially useful as photocatalysts [18,19]. However, most CPs-based photocatalyst such as ZIF-8, MOF-5 and UiO-67 can merely harvest UV light owing to the large band gap and the narrow-range adsorption which could not adsorb the light from the visible region [20,21]. To tackle this problem, some strategies such as linker decoration, dye sensing and combination with other semiconductor were adopted to reduce the band gap so as to enhance the solar light utilization [20]. Among them, a feasible way to improve the photocatalytic activity is to introduce the visible light responsive organic ligand. For instance, Li et al. successfully achieved in the synthesis of a visible-light responsive CP through substitution of benzenedicarboxylate (BDC) in UV-responsive MIL-125(Ti) by visible-light-active 2-aminoterephthalate (H_2ATA) [22]; Xing et al. have prepared a visible-light responsive CP based on a visible-light harvesting pillar [23]. Bearing these in mind, in this work, a Zn(II)/anthracene coordination polymer $[Zn(OAc)_2(BPEA)]_n$ has been successfully prepared via reaction of $Zn(OAc)_2 \cdot 2H_2O$ with a visible light responsive organic ligand 9,10-bis(4′-pyridylethynyl)-anthracene (BPEA). Compound **1** has a one-dimensional (1D) chain structure in which the binuclear $\{Zn_2(OAc)_2\}$ cores are linked by the BPEA ligands using the pyridyl N atoms to give to the 1D ladder-like network. The as-prepared compound **1** shows broad-range visible light absorption and good water stability, which are highly demandable for its application in the photocatalysis. The photocatalytic property of **1** were investigated by reduction of Cr(VI) to Cr(III) in aqueous solution under visible light, which reveals its high efficiency and stability in this photocatalytic process.

Single-crystal X-ray diffraction measurement manifests that complex **1** belongs to the triclinic space group P-1 and reveals a 1D ladder-like structure. The molecular unit of **1** contains one Zn(II) ion, one BPEA ligand and two coordinated AcO^- groups. The Zn(II) ion is six-coordinated with two N atoms from two BPEA ligands and four O atoms from three different AcO^- groups, forming a distorted octahedral geometry (Fig. 1a). The Zn(II)-N bond distances are in the range of 2.174(9) to 2.181(9) Å and the Zn(II)-O bond distances are in the range of 2.014(8) to 2.194 (1) Å. The adjacent Zn(II) ions are connected with each other via the AcO^- groups to afford the $\{Zn_2(AcO)_4\}$ secondary building unit, which is further connected by the BPEA ligands to afford the 1D ladder-like network. The 1D chains are further stabilized via the π-π interactions between the phenyl rings of the parallel BPEA ligands (Fig. 1b). Due to the tightly packed of the 1D chains, the unit cell of **1** shows no solvent accessible void as calculated via the software PLATON [24].

The phase purity of the as-prepared complex **1** has been confirmed via the PXRD measurement. As shown in the Fig. S3, the well-defined diffraction peaks revealed the high crystallinity of the products, which are in good agreement with the simulated pattern from the crystal data. In view of the following Cr(VI) reduction reactions, it is necessary to check the framework stability of **1** in water. The stability of **1** in water has been confirmed via measuring the PXRD patterns of **1** after being soaked in water for three days, which reveal good agreement with that of the as-prepared samples. The TGA curve of **1** reveals no obvious weight loss until the temperature of 287 °C, which is in accordance with that observed from the crystal data (Fig. S4). The optical absorbance of complex **1** as well as the BPEA ligand was measured by UV − vis spectrometer, which shows that the absorption edge of **1** locates at ca. 670 nm in the visible light region (Fig. 2a). Compared with the BPEA linker, the absorption band of complex **1** is obviously red-shift, probably due to the close stacking interactions between conjugated BPEA ligands in the framework of **1** [25]. The absorption spectrum of **1** is re-plotted in accordance with the frequency-dependent relationship $\alpha h\nu = (h\nu - E_g)^{1/2}$ to evaluate the band gap of **1**, where α and E_g are the absorption coefficient and the band gap energy. The plot of $(\alpha h\nu)^2$

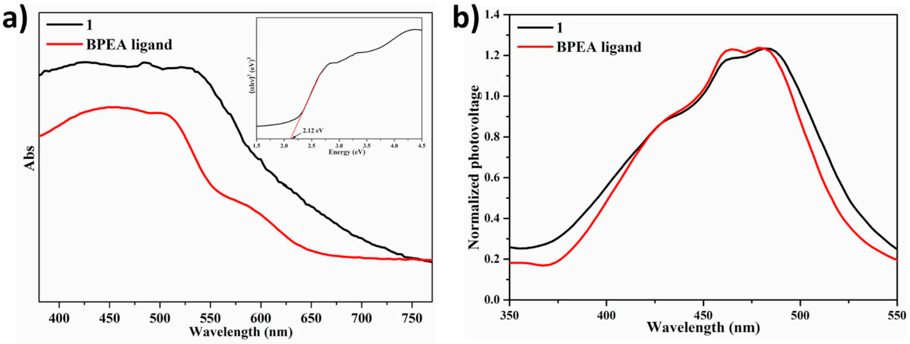

Fig. 2. (a) The UV–vis spectra for the BPEA ligand and complex **1**; (b) The SPV spectra of BPEA ligand and complex **1**.

versus photon energy displays a well-fitted linear dependence near the absorption edge, and the band gap energy of **1** is thus estimated to be ca. 2.12 eV, implying that **1** possesses the nature of semiconductivity. The SPV technique is a nondestructive approach to study heterogeneous photocatalysts by monitoring the surface voltage resulting from light-induced charge generation. As shown in Fig. 2b, complex **1** displays a wide-range SPV response from 420 nm to 550 nm with a peak at 480 nm, indicating its visible-light-induced charge generation and efficient photoinduced surface charge generation. It could be noticed that the SPV spectrum of complex **1** is similar to that of the BPEA ligand, suggesting that the photoinduced charge generation in **1** is based on the visible light responsive ligand. All the above experimental results indicate that complex **1** might serve as photocatalysts to carry out visible-light-driven photochemical reactions.

The photocatalytic activities of complex **1** were studied the reduction of Cr(VI) to Cr(III) in an aqueous solution of $K_2Cr_2O_7$ under the simulated solar light exposure. A blank experiment without a photocatalyst or sunlight was also performed to verify the concentration of Cr (VI), and the results were found to remain constant, which reflects the insignificant photolysis and relatively stable content of $K_2Cr_2O_7$ (Fig. S5). Before being exposed to light, the Cr(VI) solution was stirred in the dark at about 30 min to ensure the establishment of an adsorption – desorption equilibrium between the photocatalyst and the Cr (VI) solution. The previous study reported that the reduction rate of aqueous Cr(VI) over photocatalysts is greatly influenced by pH values of the solution and the hole scavenger [26]. In the present study, the pH value of the reaction system was adjusted by H_2SO_4 (aq, 0.2 M) and 0.2 mL of MeOH was used as the hole scavenger. As shown in Fig. 3, it can be seen that the photo-reduction efficiencies of Cr(VI) were greatly improved by the decreasing the pH values. When the pH value in the solution decrease from 7 to 4, the reduction ratio of Cr(VI) increase rapidly from 23% to 92% under the same irradiation time. This result of the experiment is consistent with other reports on aqueous reduction of Cr(VI) by CP-based photocatalysts. When the pH value was adjusted to 3, nearly 96% of the Cr(VI) in the solution could be reduced after 30 min. Compared with reported CP-based photocatalysts for Cr(VI) reduction, complex **1** has the following advantages such as it does not need the high energy UV light and it does not need to be composite with other semiconductor materials [27–29]. The stability is also of great importance to evaluate the photocatalyst. Fig. S6 shows the durability of complex **1** toward the reduction of Cr(VI) to Cr(III) under visible-light illumination. The photocatalytic activity of **1** does not obviously decrease after four cycles, showing that complex **1** exhibits high catalytic stability. Furthermore, the framework integrality after photocatalytic process has also been confirmed via the PXRD measurements. These results suggest that complex **1** shows good catalytic reusability and stability in this photocatalytic reaction.

On the grounds of all the experimental results and associate studies, a possible mechanism for the enhanced photoactivity of Cr(VI) reduction can be proposed [26–29]. As illustrated in Fig. 4, when the visible light irradiates, the BPEA ligands adsorb light and the electrons (e −) in the valance band (VB) of are easily photoexcited to the conduction band (CB), leaving the holes (h +) in the VB. Then the photogenerated electrons in the CB are transferred to reduce the Cr(VI) ions on the surface of while the holes oxidize the hole scavenger MeOH to form CO_2 and H_2O.

In conclusion, by utilizing a visible light responsive organic ligand 9,10-bis(4′-pyridylethynyl)-anthracene (BPEA), we have successfully achieved a one-dimensional (1D) chain structure which shows broad-range visible light absorption and good water stability. The photocatalytic property of **1** were investigated by reduction of Cr(VI) to Cr (III) in aqueous solution under visible light, which reveals its high efficiency and stability in this photocatalytic process. This work also highlights the importance of the visible light responsive organic ligand in the construction of CP-based photocatalyst.

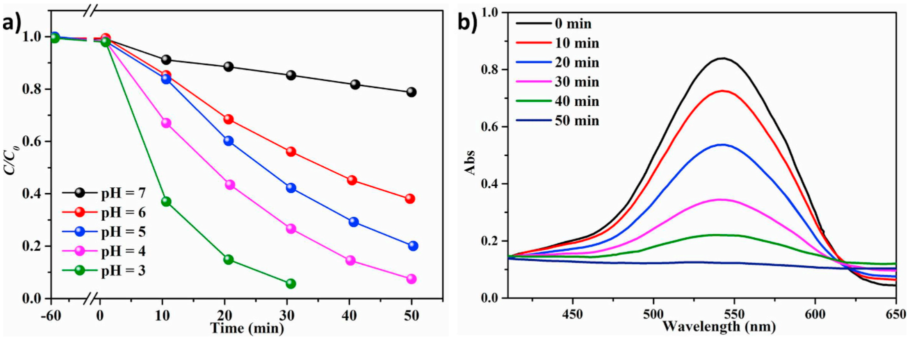

Fig. 3. (a) Reduction profiles of photocatalytic reduction of Cr(VI) over **1** under different pH conditions; (b) The UV–vis spectra for the photocatalytic reduction of Cr (VI) at pH value of 4.

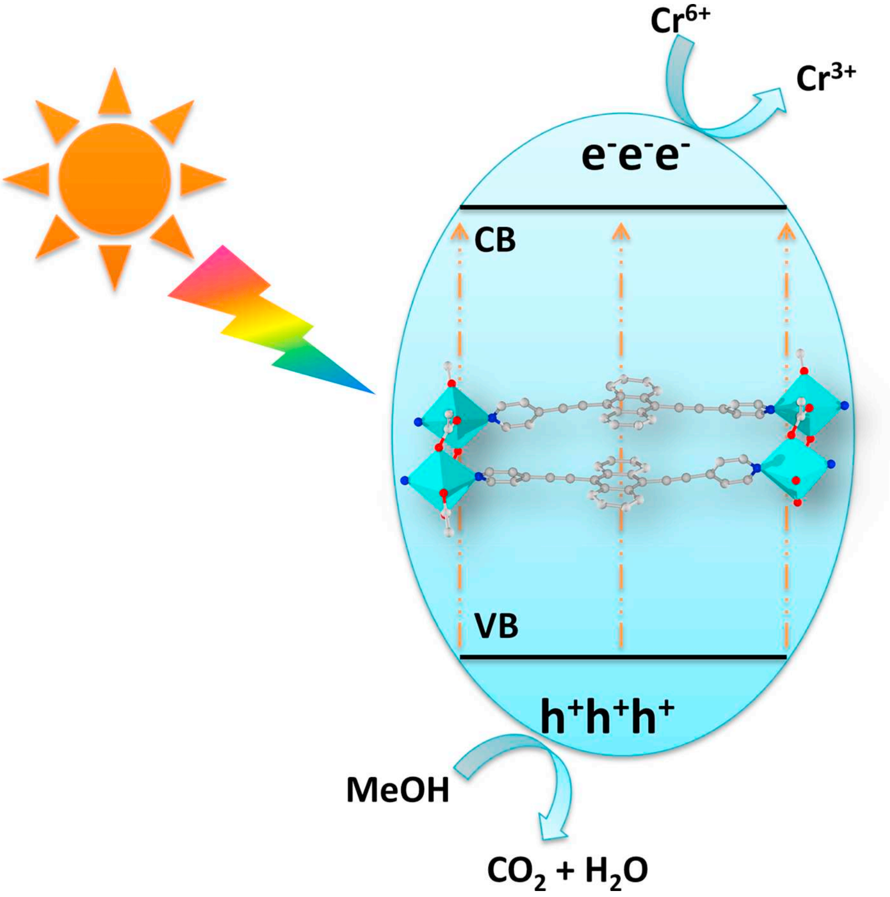

Fig. 4. Schematic illustration of photocatalytic reduction Cr(VI) over **1** under visible light irradiation.

Appendix A. Supplementary material

CCDC 1880705 (**1**) contains the supplementary crystallographic data for the title compound. This data can be obtained free of charge via http://www.ccdc.cam.ac.uk/conts/retrieving.html, or from the Cambridge Crystallographic Data Centre, 12 Union Road, Cambridge CB2 1EZ, UK; fax: (+44) 1223-336-033; or e-mail: deposit@ccdc.cam.ac.uk. Supplementary data associated with this article can be found, in the online version, at https://doi.org/10.1016/j.inoche.2019.01.006

References

[1] Y. Lu, S. Song, R. Wang, Z. Liu, J. Meng, A.J. Sweetman, A. Jenkins, R.C. Ferrier, H. Li, W. Luo, T. Wang, Impacts of soil and water pollution on food safety and health risks in China, Environ. Int. 77 (2015) 5–15.
[2] S. Satyro, M. Race, F. Di Natale, A. Erto, M. Guida, R. Marotta, Simultaneous removal of heavy metals from field-polluted soils and treatment of soil washing effluents through combined adsorption and artificial sunlight-driven photocatalytic processes, Chem. Eng. J. 283 (2016) 1484–1493.
[3] P. Yuan, M. Fan, D. Yang, H. He, D. Liu, A. Yuan, J. Zhu, T. Chen, Montmorillonite-supported magnetite nanoparticles for the removal of hexavalent chromium [Cr(VI)] from aqueous solutions, J. Hazard. Mater. 166 (2009) 821–829.
[4] F. Jing, R. Liang, J. Xiong, R. Chen, S. Zhang, Y. Li, L. Wu, MIL-68(Fe) as an efficient visible-light-driven photocatalyst for the treatment of a simulated waste-water contain Cr(VI) and Malachite Green, Appl. Catal. B Environ. 206 (2017) 9–15.
[5] B. Gu, J. Chen, Enhanced microbial reduction of Cr(VI) and U(VI) by different natural organic matter fractions, Geochim. Cosmochim. Acta 67 (2003) 3575–3582.
[6] C.E. Barrera-Díaz, V. Lugo-Lugo, B. Bilyeu, A review of chemical, electrochemical and biological methods for aqueous Cr(VI) reduction, J. Hazard. Mater. 223–224 (2012) 1–12.
[7] C.C. Wang, X.D. Du, J. Li, X.X. Guo, P. Wang, J. Zhang, Photocatalytic Cr(VI) reduction in metal-organic frameworks: a mini-review, Appl. Catal. B Environ. 193 (2016) 198–216.
[8] M. Pan, W.M. Liao, S.Y. Yin, S.S. Sun, C.Y. Su, Single-phase white-light-emitting and photoluminescent color-tuning coordination assemblies, Chem. Rev. 118 (2018) 8889–8935.
[9] W.M. Liao, C.J. Li, X. Wu, J.H. Zhang, Z. Wang, H.P. Wang, Y.N. Fan, M. Pan, C.Y. Su, Homometallic Ln(iii)-complexes from an ILCT ligand with sensitized vis-NIR emission, excitation-dependent PL color tuning and white-light emission, J. Mater. Chem. C 6 (2018) 3254–3259.
[10] Q.Y. Yang, K. Wu, J.J. Jiang, C.W. Hsu, M. Pan, J.M. Lehn, C.Y. Su, Pure white-light and yellow-to-blue emission tuning in single crystals of Dy(iii) metal–organic frameworks, Chem. Commun. 50 (2014) 7702–7704.
[11] S. Zhang, H. He, F. Sun, N. Zhao, J. Du, Q. Pan, G. Zhu, A novel adenine-based zinc (II) metal-organic framework featuring the Lewis basic sites for heterogeneous catalysis, Inorg. Chem. Commun. 79 (2017) 55–59.
[12] Y.X. Li, Z.Y. Wei, L. Liu, M.L. Gao, Z.B. Han, Ag nanoparticles supported on UiO-66 for selective oxidation of styrene, Inorg. Chem. Commun. 88 (2018) 47–50.
[13] D.F. Chai, M. Wang, C. Zhang, F. Ning, W. Xu, H. Pang, H. Ma, A novel 3D POMOF based on dinuclear copper (II)-oxalate complexes and Keggin polyoxoanions with excellent photocatalytic activity, Inorg. Chem. Commun. 83 (2017) 16–19.
[14] J.Q. Liu, G.P. Li, W.C. Liu, Q.L. Li, B.H. Li, R.W. Gable, L. Hou, S.R. Batten, Two unusual nanocage-based Ln-MOFs with triazole sites: highly fluorescent sensing for Fe^{3+} and $Cr_2O_7^{2-}$, and selective CO_2 capture, Chem. Aust. 81 (2016) 1299–1304.
[15] B.H. Li, J. Wu, J.Q. Liu, C.Y. Gu, J.W. Xu, M.M. Luo, R. Yadav, A. Kumar, S.R. Batten, A luminescent zinc(II) metal-organic framework for selective detection of nitroaromatics, Fe^{3+} and CrO_4^{2-}: a versatile threefold fluorescent sensor, Chem. Aust. 81 (2016) 885–892.
[16] J. Wang, X.R. Wu, J.Q. Liu, B.H. Li, A. Singh, A. Kumar, S.R. Batten, An uncommon (5,5)-connected 3D metal organic material for selective and sensitive sensing of nitroaromatics and ferric ion: experimental studies and theoretical analysis, CrystEngComm 19 (2017) 3519–3525.
[17] A. Ma, J. Wu, Y. Han, F. Chen, B.H. Li, S. Cai, H. Huang, A. Singh, A. Kumar, J.Q. Liu, Rational synthesis of a luminescent uncommon (3,4,6)-c connected Zn(ii) MOF: a dual channel sensor for the detection of nitroaromatics and ferric ions, Dalton Trans. 47 (2018) 9627–9633.
[18] M. Cai, G.E. Wang, M. Yao, G. Wu, Y. Li, G. Xu, Semiconductive 1D nanobelt iodoplumbate hybrid with high humidity response, Inorg. Chem. Commun. 93 (2018) 42–46.
[19] W.M. Liao, J.H. Zhang, Z. Wang, Y.L. Lu, S.Y. Yin, H.P. Wang, Y.N. Fan, M. Pan, C.Y. Su, Semiconductive amine-functionalized Co(II)-MOF for visible-light-driven hydrogen evolution and CO_2 reduction, Inorg. Chem. 57 (2018) 11436–11442.
[20] M.A. Nasalevich, M. van der Veen, F. Kapteijn, J. Gascon, Metal–organic frameworks as heterogeneous photocatalysts: advantages and challenges, CrystEngComm 16 (2014) 4919–4926.
[21] W.M. Liao, J.H. Zhang, Z. Wang, S.Y. Yin, M. Pan, H.P. Wang, C.Y. Su, Post-synthetic exchange (PSE) of UiO-67 frameworks with Ru/Rh half-sandwich units for

visible-light-driven H_2 evolution and CO_2 reduction, J. Mater. Chem. A 6 (2018) 11337–11345.

[22] D. Sun, Y. Fu, W. Liu, L. Ye, D. Wang, L. Yang, X. Fu, Z. Li, Studies on photocatalytic CO_2 reduction over NH_2-Uio-66(Zr) and its derivatives: towards a better understanding of photocatalysis on metal-organic frameworks, Chem. Eur. J. 19 (2013) 14279–14285.

[23] Y. Liu, D. Chen, X. Li, Z. Yu, Q. Xia, D. Liang, H. Xing, Visible-light-induced controlled radical polymerization of methacrylates mediated by a pillared-layer metal–organic framework, Green Chem. 18 (2016) 1475–1481.

[24] A.L. Spek, Acta Crystallogr. Sect. A: Found. Crystallogr. 46 (1990) C34.

[25] X. Liang, Z. Guo, H. Wei, X. Liu, H. Lv, H. Xing, Selective photooxidation of sulfides mediated by singlet oxygen using visible-light-responsive coordination polymers, Chem. Commun. 54 (2018) 13002–13005.

[26] H. Zhao, Q. Xia, H. Xing, D. Chen, H. Wang, Construction of pillared-layer MOF as efficient visible-light photocatalysts for aqueous Cr(VI) reduction and dye degradation, ACS Sustain. Chem. Eng. 5 (2017) 4449–4456.

[27] D.M. Chen, C.X. Sun, C.S. Liu, M. Du, Stable layered semiconductive Cu(I)–organic framework for efficient visible-light-driven Cr(VI) reduction and H_2 evolution, Inorg. Chem. 57 (2018) 7975–7981.

[28] J. Qiu, X.F. Zhang, X. Zhang, Y. Feng, Y. Li, L. Yang, H. Lu, J. Yao, Constructing Cd 0.5 Zn 0.5 S@ZIF-8 nanocomposites through self-assembly strategy to enhance Cr (VI) photocatalytic reduction, J. Hazard. Mater. 349 (2018) 234–241.

[29] Y. Pi, X. Li, Q. Xia, J. Wu, Z. Li, Y. Li, J. Xiao, Formation of willow leaf-like structures composed of NH_2-MIL68(In) on a multifunctional multiwalled carbon nanotube backbone for enhanced photocatalytic reduction of Cr(VI), Nano Res. 10 (2017) 3543–3556.